Int J Adv Manuf Technol (2007) 33:86–94
DOI 10.1007/s00170-007-0968-1

ORIGINAL ARTICLE

Patterned crack-free PZT thick films for micro-electromechanical system applications

F. Dauchy · R. A. Dorey

Received: 16 January 2006 / Accepted: 26 January 2007 / Published online: 16 March 2007
© Springer-Verlag London Limited 2007

Abstract The fabrication and structuring of multilayer-thick film piezoelectric (PZT-lead zirconate titanate) structures, using composite sol-gel techniques and wet etching is described. The composite sol-gel technique involves producing a PZT powder/sol composite slurry which when spun down, yields films a few micrometres thick. Repeated layering and infiltration has been used to produce PZT films between 10 and 40 μm thick. Due to the low firing temperature (<720°C), it has also been possible to produce PZT films with embedded thin (ca. 100 nm thick) metal electrodes. The PZT thick films have also been structured using a wet etching technique. Examples of features and cavities with lateral dimensions in the order of tens of micrometres are presented. The ability to fabricate and structure thick functional films with embedded metal electrode structures offers the possibility to create novel micro-device structures suitable for use in micro-electro-mechanical systems (MEMS).

Keywords Sol gel · Thick film · MEMS · Multilayer

1 Introduction

Ferroelectric thick films can be developed for inclusion in MEMS technology for the fabrication of transducers working in thickness mode. These devices can be made from polycrystalline ceramics. This involves two fabrication steps: preparation of the green ceramic and sintering. A PZT powder/fluid (water, oil or alcohol) slurry allows one to deposit films with thickness ranging from micrometres to millimetres via several methods such as tape casting (up to millimetres) [1, 2], and screen printing (up to hundreds of microns) [3, 4]. Unfortunately, the powder route must have a high-temperature sintering stage, typically above 1,200°C, and also presents many technical difficulties to achieve the fabrication of uniform films tens of micrometres thick.

For piezoelectric applications, wet chemical methods (sol-gel) are used due to their very low sintering temperature (600°C), which allows the films to be integrated onto substrates such as silicon. A second advantage is the grain uniformity in terms of size distribution and composition that this technique gives, which is a key factor needed to achieve reproducibility of piezoelectric characteristics. However, a pure sol-gel technique only gives films with a maximum thickness of ca. 3 μm [5]. The main challenge is to fabricate PZT thick films with a thickness ranging from 10 to 40 μm and to keep the advantage of the low sintering temperature of the sol-gel method.

A mix between the two techniques presented allows these conditions to be met. A composite PZT powder/sol slurry used in our work can be spun to achieve different thicknesses ranging from 2 μm up to 35 μm with a sintering process at 720°C. This is a good trade-off between a powder route and a pure sol-gel procedure. The thickness of 35 μm for single or multilayer structures are state of the art and are suitable for several new industrial applications such as transducers for high-frequency imaging using the thickness mode of excitation. The spin coating technique was chosen for deposition because it offers a greater flexibility in thickness, even if this range of thickness for spun PZT films have not previously been made [6]. This paper summarises the process required to go from the sol gel through to the final shaped structures.

F. Dauchy (✉) · R. A. Dorey
Microsystems and Nanotechnology Centre,
School of Applied Sciences, Cranfield University,
Cranfield, Bedfordshire MK43 OAL, UK
e-mail: f.dauchy.2003@cranfield.ac.uk

2 PZT sol-gel and composite slurry

2.1 PZT sol-gel

The general formula of the sol used was: $Pb_{1.1}[Nb_{0.02}Sb_{0.02}Mn_{0.02}(Ti_{0.48}Zr_{0.52})_{0.94}]O_3$ [7]. Figure 1 shows the fabrication steps of the sol. The 2-methoxy-ethanol and the lead-acetate solution were mixed together and the resulting solution was refluxed under N_2 to drive the hydrolysis polymerisation. At this stage, the solution was cloudy. The synthesis was completed by a long final distillation to remove the by-products. A first plateau is observed at 90°C, which corresponds to the boiling point of propanol used as a solvent to stabilize the zirconium propoxide. A second plateau is observed at 102–104°C to physically remove the water. The sol becomes yellow and clear. The amount of solution removed during the final distillation is replaced by the same amount of 2-methoxy-ethanol to reach a concentration of 1.1 M. The sol is then filtered and stabilized by the addition of ethyl glycol [8].

2.2 Composite slurry

A sol-gel method combined with PZT powder will be useful for thick film deposition. During the sintering process, atomic diffusion in the PZT powder grain occurs to minimise the surface energy, which promotes crystal bonding at the interface between two adjacent particles. The added sol will increase the driving force of the system due to the presence of nanoscale particles and so lower the required sintering temperature. In addition, the sol will also function as a glue, binding the larger particles together and to the substrate.

Table 1 Composition of the composite slurry

PZT powder (PZ 26, Ferroperm, DK)	45 g
Dispersant KR 55 (Ken React Lica 38, IPA isooctyl alcohol)	0.9 g
PZT sol	30 ml
Sintering aid Cu_2O/PbO	0.3105 g/1.926 g
Zirconia ball-milling media	200 g

With a pure sol-gel route the substrate, generally, an $Si/SiO_2/Pt$ wafer will be the “seed” inducing the crystallisation. In the case of the composite sol-gel route, each microsize PZT grain will act as a site for crystallization. The composition of the composite slurry is summarised in Table 1. All of the components were mixed together under nitrogen in a 125-ml flask. The slurry was then ball-mixed for 24 h to produce a stable suspension. The slurry obtained has a density of 2.2 $g.ml^{-1}$.

To enhance densification of the film, a small amount of sintering aid Cu_2O-PbO[9] was added. This sintering aid forms a low-temperature liquid phase during the sintering process and accelerates the atomic diffusion at the grain surface [9], further increasing the density of the ceramic. The composite slurry is sintered at 720°C following patterning [10].

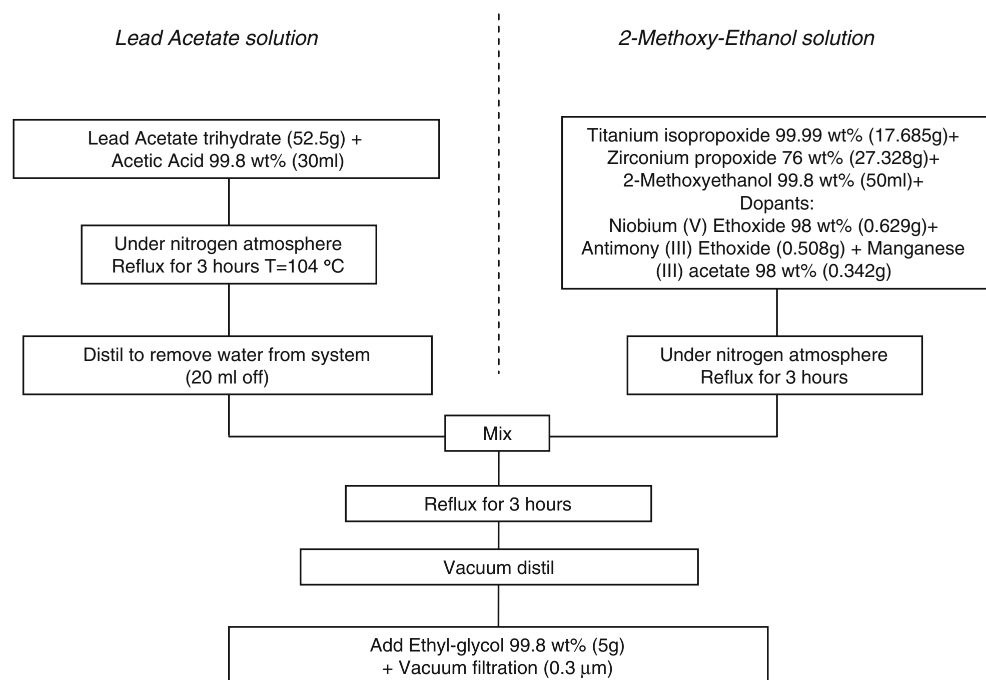

Fig. 1 Flow chart showing the fabrication steps used to produce the PZT sol

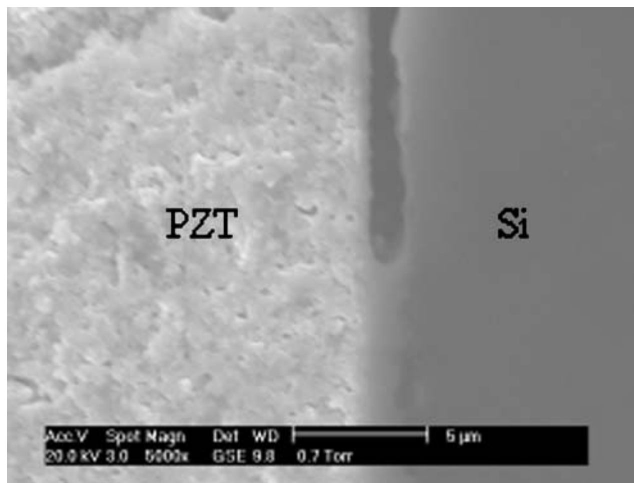

Fig. 2 Holes produced at the Si/PZT interface due to diffusion of the Pb into the Si substrate during sintering

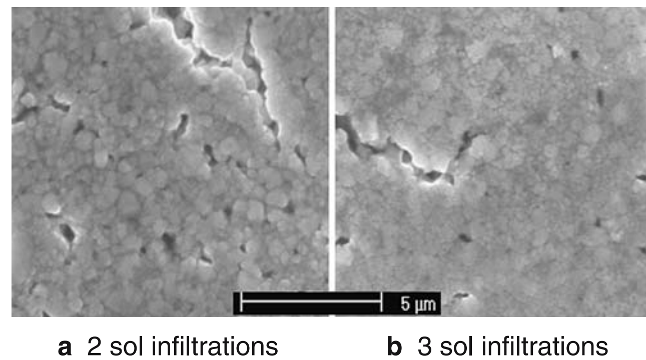

Fig. 3 SEM micrograph of the surface of a PZT film showing how increased sol infiltration results in a reduction of porosity

3 PZT deposition

During the sintering process, some Pb from the PZT layer diffuses into the silicon wafer substrate to form lead silicate that is liquid at the sintering temperature (Fig. 2).

To prevent this undesirable reaction, a ZrO_2 diffusion barrier (Table 2) was first spun on the silicon substrate.

These components were mixed under nitrogen and stirred for 1 h. The sol was spun at 3,000 rpm for 30 s and dried at 350°C. This stage was repeated three times. The film was then sintered at 800°C for 10 min, resulting in a final thickness of 60 nm.

Sputtered Pt bottom electrodes were then shaped with a liftoff process. The photoresist S1818 was spun at 4,000 rpm, dried for 90 s at 115°C, partially exposed under UV light for 10 s, and then developed in MF319 developer. An adhesion layer of PZT sol was spun before spinning the composite slurry in order to avoid any delamination. This step was done for all films thicker than 21 μm. PZT was deposited by fully coating the substrates with the composite suspension and then spinning at 2,000 rpm for 30 s. The deposited film was then dried at 200°C for 60 s and pyrolysed at 450°C for 30 s to remove all the organic components.

Table 2 Composition of the ZrO_2 diffusion barrier sol

ZrO_2 diffusion barrier	Qty
Zirconium propoxide (75 wt% in propanol)	4.344 g
Acetic acid (at 99.8 wt%)	3 ml
Ethanol anhydrite	47 ml

4 Infiltration steps

The composite slurry process, even when using the sintering aid, still results in a low-density film after sintering. This was overcome by repeated sol infiltration to increase the green density prior to sintering. An infiltration step consists of spinning a layer of a sol, diluted in 2 methoxy-ethanol (2 ME) solution, on the green ceramic (1:1 sol: 2 ME). The added sol will directly crystallise in the pores and fill them. This increase in density is shown in Fig. 3 and confirmed by an increase in the relative permittivity with the number sol infiltrations (Fig. 4).

Each infiltration step was followed by drying and pyrolysis treatments at 200 and 450°C, respectively, before the next infiltration step. The next composite layer was then deposited and the process was repeated until the desired thickness was obtained. The sample notation use throughout this article is x [yC + zS], where: "y" represents a number of composite layers spun, "z" represents the number of infiltrations per "yC" composite layer, and "x" represents the number of times the unit [yC + zS] is realised to achieve the required thickness.

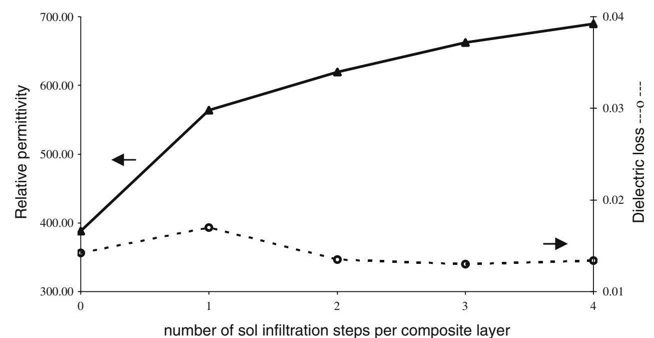

Fig. 4 Variation in relative permittivity and dielectric loss of 4[C+xS] as a function of sol infiltration

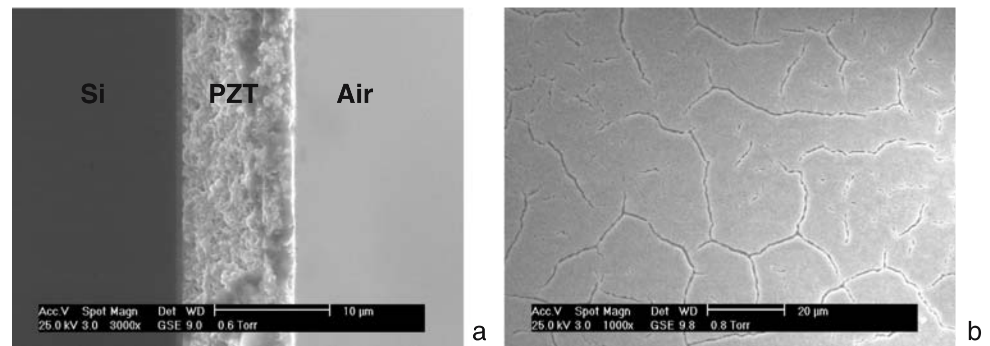

Fig. 5 SEM micrograph of 10-µm PZT thick film composed of 4[C+4S], cross section (**a**), surface (**b**)

5 Unpatterned crack-free thick film

5.1 Thick film [C+4S]

The substrate ($Si/SiO_2/ZrO_2$/PZT sol) enabled 16 composite layers to be spun to achieve a thickness of 35 µm, which is state of the art for a spin-coated PZT ceramic and has not previously been reported. Figures 5, 6 and 7, represent the evolution of the surface with the thickness. The surface finish of films composed of 12 or more composite layers shows some cracking. The width of these cracks can be reduced to tens of nanometres by covering the surface with a pure sol (Fig. 7b). This step allows the ceramic to be used for MEMS applications as a continuous top electrode as thin as 100 nm and can be sputtered on the surface.

The cross section (Fig. 6a) reveals that some of the four infiltration steps do not completely infiltrate the composite layer. Some of the infiltration sol remains on the surface of each composite layer, which marks the observable separation between the two (Fig. 6). This effect is also observable during the wet etching process. Figure 14 shows a stepped pyramidal shape due to the presence of this interlayer sol.

The work presented by [12] on pure sol demonstrates that the interfacial sol layer is far denser than the composite ceramic. These density differences may induce a considerable amount of tensile stress due to the differential shrinkage during the drying stage, which may lead the composite film to crack and delaminate. Experimentally, the cracks appeared during the drying stage at 200°C, and especially when the infiltration sol did not totally infiltrate the PZT, indicating that the drying/shrinkage of the pure sol plays a significant role in this process. A trade-off between dielectric properties and a better surface finish can be made. To do so, some infiltration stage causing the interfacial PZT layer can be eliminated along with the accompanying stress, which will lead to a crack-free thick PZT film.

5.2 Thick film [2C+4S]

The process [2C+4S] corresponds to two infiltration steps per composite layer. The infiltration sol remaining between the two composite layers (observable in Fig. 7) is not observable with the new process (Fig. 8). The cracking situation is improved significantly even for a thick layer of 28 µm where the surface finish remains better than for a 10-µm-thick film for the first process [C+4S]. Such a reduction in cracking would arise either due to a reduction in stress or an increase in material strength. However, as strength is expected to decrease with increasing porosity, it is reasonable to assume that the cracking is eliminated in these (more porous) films due to a reduction in stress. (Figs. 8 and 9).

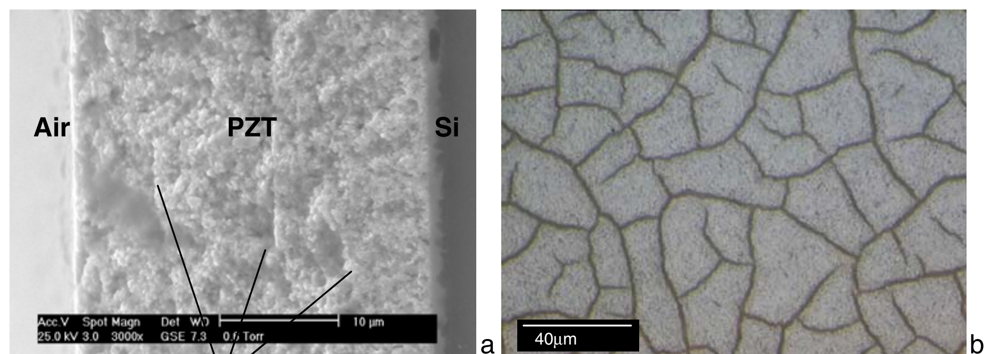

Fig. 6 **a** SEM micrograph of a 25-µm PZT thick film composed of PZT 12[C+4S]. The cross section highlights the boundary between composite layers caused by the infiltration stage. **b** Light microscope image of surface of this thick film showing increase in scale of cracking

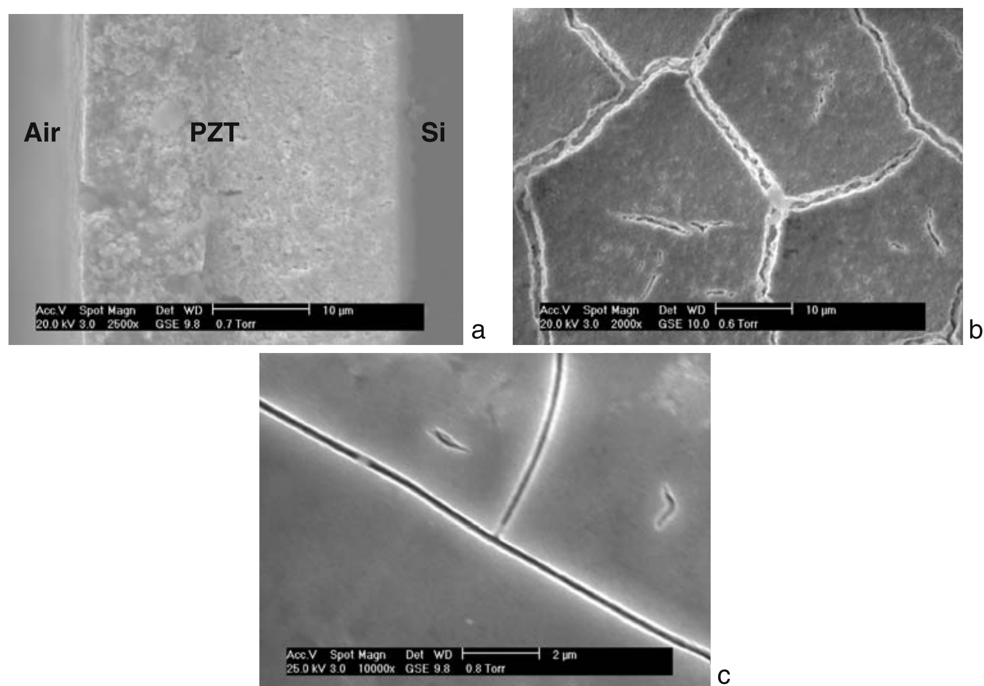

Fig. 7 SEM micrograph of 35-μm PZT thick film composed of 16[C+4S]. **a** Cross section. **b** Surface. **c** Surface of the same film coated with one layer of pure PZT sol showing reduction in crack width

It is expected that these ceramics contain higher porosity than the x[C+4S] ceramics, as they have been infiltrated to a lesser degree. As a consequence, the relative permittivity is reduced from 700 to 630–600. However, this process represents a real breakthrough regarding the thickness (28 μm) of such thick films, as well as for the surface finish achievable. As an example of the quality of surface finish achievable with this process, Fig. 8a represents a 22-μm crack-free thick PZT film with a 100-nm electrode sputtered on its surface, showing that a continuous electrode can be deposited. An investigation into the roughness of the PZT thick film surface was performed using a VEECO Dektak stylus profiler, which demonstrates that a 30-nm roughness of the PZT thick film surface finish is achieved. This surface roughness limits the top electrode thickness at a minimum of 40 nm. However, this roughness is also an important factor for the top electrode adhesion. Therefore, the top electrode thickness standard was chosen as 100 nm (Fig. 8).

6 Multilayer PZT thick film

The composite sol-gel process offers the potential for great adaptability for thick fabrication, particularly for shaping the final device. An example of the adaptability is the PZT thick film multilayer structure with embedded electrode as shown in Fig. 10.

This device is composed of two layers each made up of seven spun composite layers infiltrated four times. The top, bottom and middle Ti (9 nm) /Pt (100 nm) electrode were deposited by sputtering.

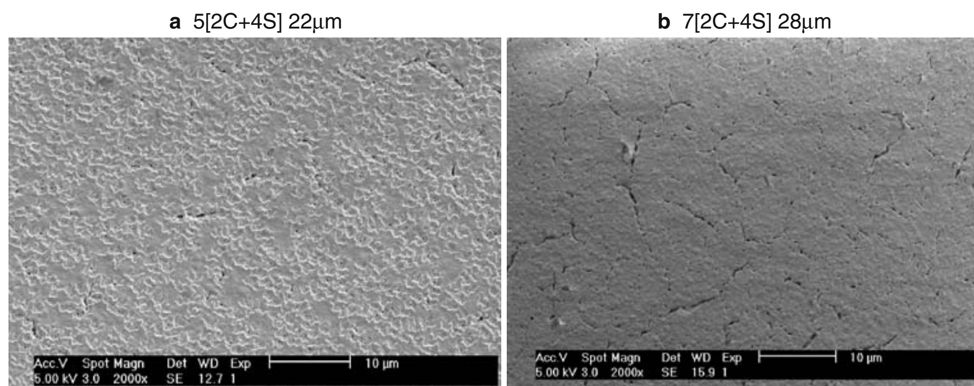

Fig. 8 SEM micrograph of surface finish of the process x [2C+4S] for two different thicknesses of film showing a marked reproduction in cracking in comparison to x[C+4S] films. **a** Shown with 100 nm of Pt sputtered the surface. **b** Virgin PZT surface

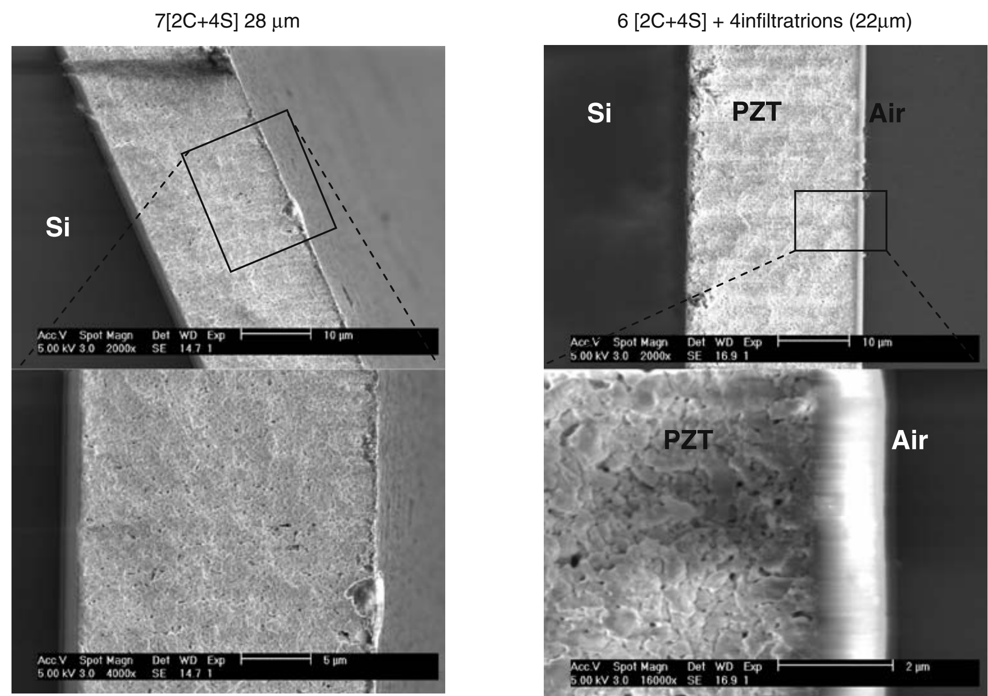

Fig. 9 SEM micrograph of cross sections of x[2C+4S] film showing the film to be more porous than the [C+4S] process shown on Fig. 6

The multilayer process shows a great adaptability in being able to deposit multiple thin (100-nm thick) metallic embedded electrodes in a PZT Structure.

7 Patterning

7.1 Wet etching solution

The solution used to etch the green ceramic was an HF/HCl solution with the following composition [HF (0.5 vol%), HCl (4.5 vol%), H_2O (95 vol%)]. To be efficient, the solution was held at 60°C during the procedure.

7.2 Patterning PZT thick films via wet etching

7.2.1 Wet etching of x[C+4S] PZT thick films

Considering the isotropy of the PZT thick film, a wet etching technique should etch at the same rate in all the directions, which explains the etching slope, called undercuts, shown in Figs. 11 and 12. The immersion time in the etch solution was dependent upon the thickness of the PZT (Table 3).

There was an intermediate product produced during the process. When the PZT was etched, a white layer was left

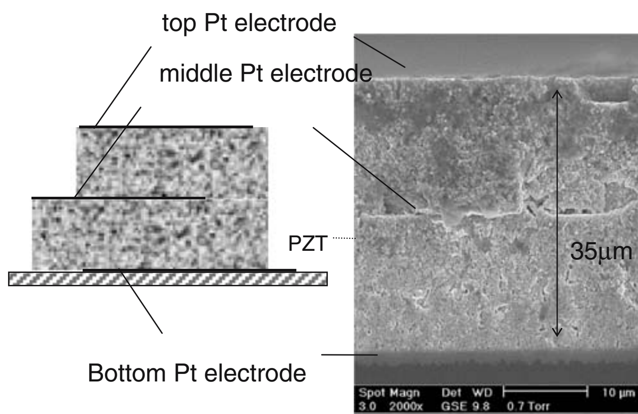

Fig. 10 Schematic and SEM image of a multilayer PZT thick film 14 [C+4S] with embedded electrode after the seventh composite layer

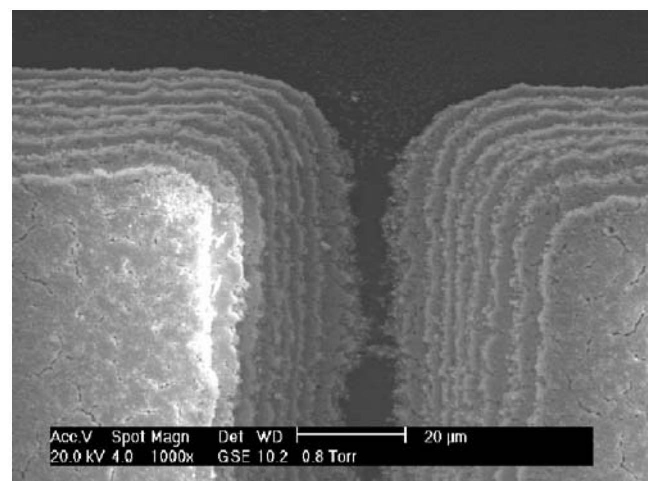

Fig. 11 SEM micrograph of a 21-μm PZT thick film patterned with features of 10 μm at the base

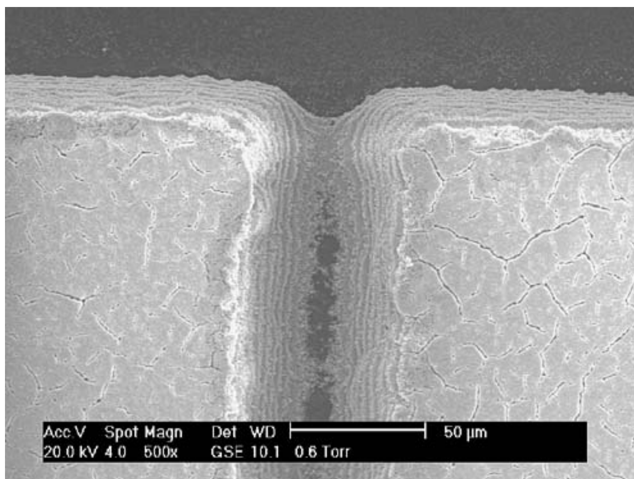

Fig. 12 SEM micrograph of a 30-µm PZT thick film patterned with features of 50 µm at the surface and 10 µm at the base

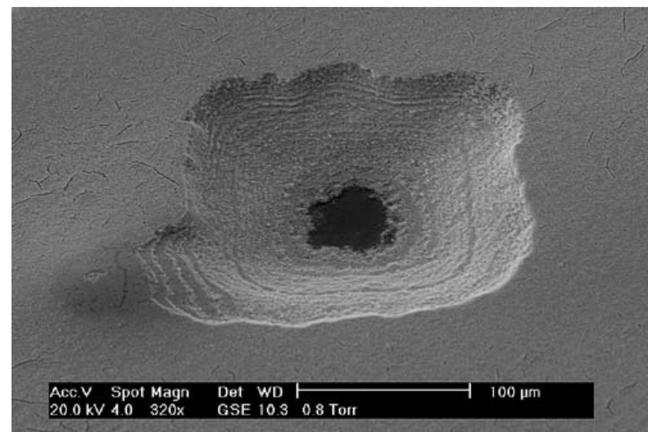

Fig. 13 SEM micrograph of a 150-µm hole PZT in a 35-µm-thick PZT film produced using mask with a 110-µm aperture. The defect near the bottom left of the hole is due to delamination of the photoresist and subsequent overetching

on the surface. An XRD study on wet etching done by Zheng [11] indicated that it was PbClF. In order to remove this residue, the sample was cleaned using water in an ultrasonic bath for 15 min at the end of the etching process.

Table 3 reveals that thicker films with more residue show reduced etching rates, which indicates that the PbClF residue acts as a barrier that slows the etching process.

The edge resolution as well as the etching slope observed in all of the present pictures seems to be dependent on the thickness and uniformity of the spun photoresist and the immersion time in the HF solution. The spinning process of the photoresist was conducted in one stage for the sample shown in Fig. 11 and two stages for that shown Fig. 12. For the 21-µm-thick sample, the resist was spun at 4,000 rpm for 1 min, while for the 30-µm-thick sample, the resist was spun first at 600 rpm for 1 min and then at 4,000 rpm for 1 min. The undercut seems to be reduced in the second case. Figure 11 shows an etching slope of 0.7 and Fig. 12 shows a slope of 1. The thicker the resist is, the longer the photoresist takes to be removed by the HF solution, and the sharper the etching slope achieved is.

Figures 11 and 12 represent the typical gap between two devices achievable by this wet etching technique. A kerf of ~60 µm between surfaces is shown in Fig. 12 for a 30-µm PZT thick film. This result is the finest result achievable with a wet etching technique considering the thickness and the isotropy of the film. The gap of 10 µm between features at the silicon face is also of technical interest (Fig. 11). A hole with 150 µm side at the surface of a 35-µm-thick film shows the capability that the wet etching technique can achieve considering that (Fig. 13):

- The photoresist patterning mask is designed with a hole with 110-µm-long sides
- A minimum of 35 µm undercuts with an isotropic wet etching technique

7.2.2 Wet etching of PZT thick film [2C+4S]

The same wet etching process was tested on [2C+4S] thick films to determine how the absence of the sol interlays affects the etch process (Table 4).

The data comparison presented in Tables 3 and 4 demonstrates a faster etching rate for the second process than for the first. This result is consistent with the porosity assumption made in Section 5 where the porosity increases when the film is less infiltrated. With a more porous film, the HF solution can have a larger reaction surface with the PZT.

Table 3 PZT etch rate for different thicknesses of PZT film etched (HF (0.5 vol%), H_2O (95 vol%), HCl (4.5 vol%)

Time to etch through thickness (min)	Thickness (µm)	Etch rate (µm/min)
7	21	3
12	30	2.5
15	35	2.3

Table 4 HF etching rate of the PZT thick film lead by the [2C+4S] process

	Time (min)	Thickness (µm)	Etch rate (µm/min)
5[2C+2S]	5.30	22	4.2
6[2C+2S] +4	Inf 6.15	22	3.6
7[2C+2S]	6.50	26	4

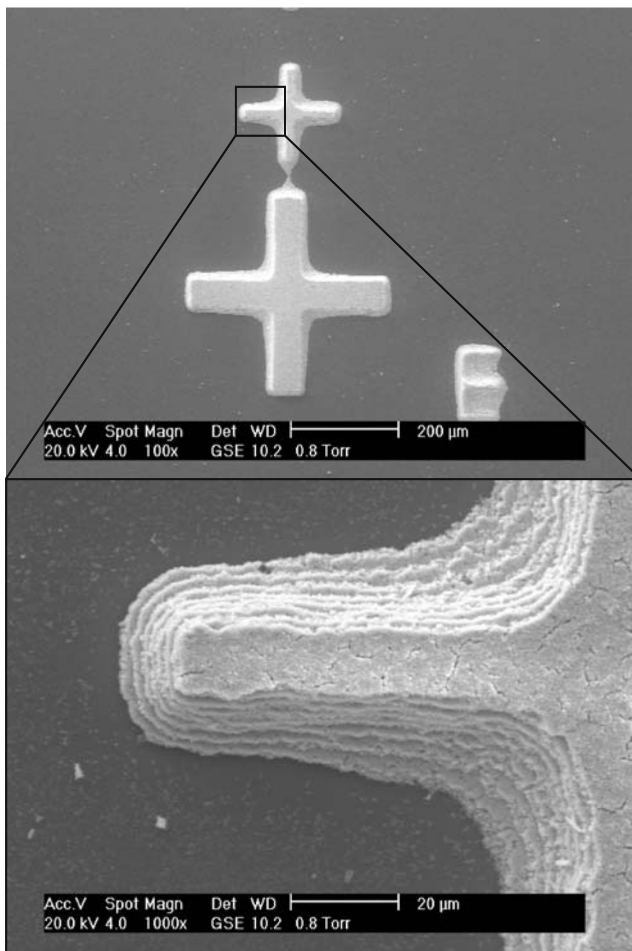

Fig. 14 SEM micrograph of a 21-µm PZT thick film, patterned to produce a 10-µm-wide feature

However, the “stepped pyramidal” etching shape observable in the first process (Figs. 12, 14 [C+4S]) is no longer observed with the second process (Figs. 6, 15 [2C+4S]) as the interlayer sol is no longer present (see Section 5.2). The higher density of the extra sol layer observed on Fig. 14 temporarily slows the through thickness etching rate (acting like a very thin protection layer against the etching solution) resulting in the stepped structure.

For a similar thickness, the etching slope is steeper for the first process than for the second one (Fig. 15). Both the porosity and the interfacial sol layer are responsible of this difference. Unfortunately, as these two variables change together it is impossible to tell which has a major effect through this experiment.

This great adaptability of the spin-coated thick composite PZT layer allows a wide range of shapes to be realised. Some examples given are state of the art and can find application in various areas. The cross shown in Fig. 14 reveals the possibility of patterning a 10-µm-wide bar of 21 µm PZT thick film, which is a significant achievement over previous techniques. Both the surface finish and the dielectric properties are tuneable for any thickness up to 40 µm. These processes could find many applications in MEMS fabrication for devices such as cantilevers, switches and high-frequency transducers.

8 Conclusions

PZT films up to 35 µm thick were fabricated using a composite sol-gel route combining a PZT powder and a PZT sol gel. The maximum temperature for the process was 720°C. A demonstration of single and multilayer structures was given to show the flexibility of this technology. A crack-free surface finish of a 28-µm-thick film reveals the adaptability of the spin coating technique to fabricate thick films. Wet etching technology revealed the possibility of a great adaptability to pattern and shape innovative devices such as bars 10 µm wide of 21 µm PZT thick film. The results open the way to a wide range of new industrial applications requiring small features and/or multilayer PZT thick film with embedded electrodes.

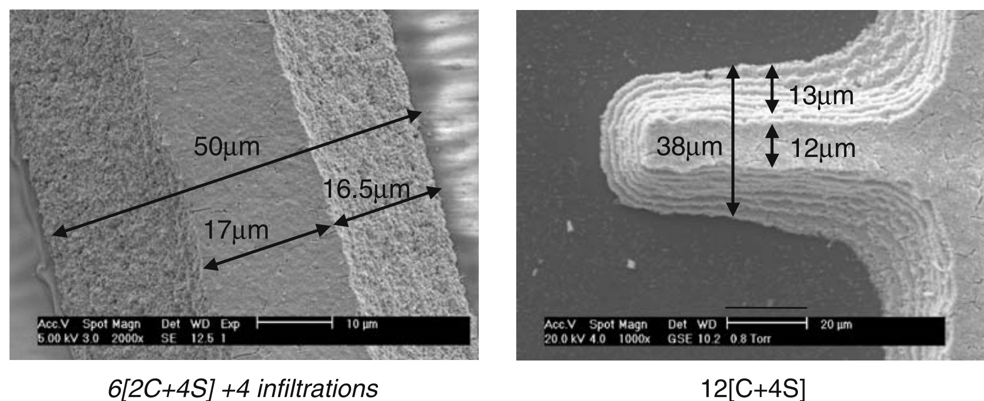

Fig. 15 Comparison between the etching definition of the two process, [2C+4S] and [C+4S]. The samples are both 21 µm thick

Acknowledgements Dr. S. A. Rocks, R. V. Wright, EC MUSTWIN project (NMP2-CT-2003-505630), Royal Academy of Engineering / EPSRC

References

1. Scharzer S, Roosen A (1999) Tape casting of piezoceramic/polymer composites. J Euro Ceram Soc 19:1007–1010
2. Liliehorn T, Johanson S (2004) Fabrication of multilayer 2D ultrasonic transducer microarrays by green machining. J Micromaching Microengineering 14:702–709
3. Simon Seveyrat L, Gonnard P (2003) Processing and characterization of piezoelectric thick films screen-printed on silicon and glass-ceramic substrates. Integr Ferroelectr 50:1–18
4. Cannell D, Trigg P (1990) Advanced ceramic processing and technology, Chap 4. Processing of electronic ceramics, pp 95
5. Ledermann N, Muralt P, Baborowski J, Gentil S, Mukati K, Cantoni M, Seifert A, Setter N (2003){1 0 0}-Textured, piezoelectric Pb(Zr*x*, Ti1-*x*)O3 thin films for MEMS: integration, deposition and properties. Sens Actuators A 105:162–170
6. Meyerhofer D (1978) Characteristics of resist films produce by spinning. J Appl Phys 49(7):3993–3997
7. Livage J, Sanchez C (1992) Sol-gel chemistry. J Non-Cryst Solids 8:145
8. Whatmore RW, Zhang Q, Huang Z, Dorey RA (2003) Ferroelectric thin and thick films for microsystems. Mater Sci Semicond Process 5:65–76
9. Dorey RA, Stringfellow SB, Whatmore RW (2002) Effect of sintering aid and repeat sol infiltration on the dielectric and piezoelectric properties of a composite thick film. J Euro Ceram Soc 22:2921–2926
10. Duval FFFC, Dorey RA, Zhang Q, Whatmore RW (2003) Lead germanium oxide sinter-assisted PZT composite thick films. J Euro Ceram Soc 23:1935–1941
11. Zheng K, Lu J, Chu J (2003) Study on wet-etching of PZT thin film. Microprocesses and nanotechnology conference international 2003. Dig Pap 29–31:248–249
12. Zhang Q, Corkovic S, Shaw CP, Huang Z, Whatmore RW (2005) Effect of porosity on the ferroelectric properties of sol-gel prepared lead titanate thin films. Thin Solid Films 488:258–264